

## Optogalvanic Detection of Negative Ions in Discharges

Takanori Suzuki and Takahiro Kasuya

Institute of Physical and Chemical Research, Hirosawa 2-1, Wako, Saitama, 351-01 Japan

Received 5 March 1990/Accepted 19 June 1990

**Abstract.** With the aid of rf, microwave and dc discharges, an optogalvanic (OG) signal, due to the photodetachment of negative oxygen ions, has been observed. The OG signal intensity in an rf discharge was successfully estimated from the discharge parameters. Thus, the OG technique may be potentially useful as a plasma diagnostic method. Furthermore, the OG signal from negative oxygen ions is found to be strong in the diffusion-controlled positive column, while the OG signal due to the excited levels of atomic oxygen is strong in the cathode fall region. Preliminary results for the observation of the OG signal in discharges of  $H_2$ , CO,  $H_2O_2$ , and  $(COCH_3)_2$  are also described.

**PACS:** 32.80Fb, 5150+v, 52.70-m

There has been considerable interest in negative-ion plasmas for a number of reasons [1, 2], such as fundamental plasma processes and because negative-ion plasmas are found in many natural and technological settings, including: the stellar atmosphere, the earth's ionosphere [1] and plasma etchants [3]. Laser optogalvanic (OG) spectroscopy [4] is a very sensitive technique in the detection of atoms and molecules in a discharge [5], and may even be a versatile optical technique for diagnosis of negative ion plasma [6].

The mechanism of laser optogalvanic effect of negative ions can be simply understood from the large difference in the mobility of the negative ions and the photodetached electrons [7]. Laser optogalvanic spectroscopy of negative ions has been successfully applied to various negative ions. In a hollow cathode dc discharge,  $I^-$  [7],  $CN^-$  [8], and  $Cl^-$  [9] have been studied and electron affinity for these species has been accurately determined from the photodetachment threshold.

In an rf discharge, negative ion kinetics are affected by the frequency of the applied oscillating field. Gottsho and Gaebe [10] observed  $Cl^-$  in a  $Cl_2$  discharge and  $BCl_3^-$  in a  $BCl_3$  discharge irradiating pulsed XeCl laser in the sheath regions of 50–750 kHz discharges. In much the same fashion, Kramer et al. [11] observed optogalvanic signals due to  $Cl^-$  by an irradiation of pulsed XeCl laser at the bulk plasma region in a 13.56 MHz  $Cl_2$  discharge.

Suzuki and Kasuya [12] observed the optogalvanic signal of  $O^-$  and  $O_2^-$  at a considerable signal-to-noise

ratio (SNR) with a cw laser in a 13.56 MHz  $O_2$  discharge, and has shown that signal intensity near the photodetachment threshold of  $O^-$  is proportional to the photodetachment cross section. The transition strengths obtained for transitions among various fine structures compare well with theoretical expectations, if the higher order correction, due to the induced dipole moment, is taken into account [13].

Glow discharges often encountered in a processing plasma or in a laboratory are grouped into dc, rf and microwave discharges according to driving frequency. Mechanisms and characteristics are different for each type of discharge [14]. In high frequency electrodeless discharges, the entire plasma is approximately neutral and diffusion-controlled, and discharge often resembles the positive column of an equivalent dc discharge, since the complications of the cathode and anode regions observed in a dc glow discharge are absent. In the positive column of electronegative gases, a space-charge sheath field between the plasma and the glass wall prevents the negative ions from diffusing to the walls, resulting in a flat radial distribution of electronegative ions in plasma [15]. The slow diffusing rate of negative ions compared to electrons results in a negative ion density approximately two orders of magnitude larger than electron density. High density and slow diffusion rate of negative ions causes instability of the oxygen discharge [14]. This correlates with the findings that both the rf and dc discharge of oxygen was sufficiently noise-free only under

the critical condition of discharge current and gas pressure, due to the ion-balance in the discharge [12, 15]. It should also be noted that these ions are too massive to carry current at an rf frequency [14]. Interpretation of the OG signal in an rf discharge is thus made simpler, since we can neglect the current carried by negative ions.

In this paper, we demonstrate the possibility of using the OG method as a diagnostic technique for discharge plasma, by successfully estimating the OG signal intensity from the measured discharge parameters. Different behavior of the OG signal of negative oxygen ions in different type of discharges is also shown, although a quantitative analysis was made only for an rf discharge. Preliminary results for the observation of OG signals, due to negative ions in discharges of other molecular gases such as  $\text{H}_2$ ,  $\text{CO}$ ,  $\text{H}_2\text{O}_2$ , and  $(\text{CQCH}_3)_2$ , are also presented.

## 1. Experimental

### 1.1. RF Discharge

Experimental details of the rf optogalvanic detection method [16] used in our studies have been described in detail elsewhere [12]. Briefly, an rf electric field at 13.56 MHz is applied across a Pyrex discharge tube (10 mm outside diameter) by two copper rings attached to the tube. Commercial  $\text{O}_2$  gas is continuously supplied to the discharge tube. Measurement of photodetachment in oxygen was carried out under a critical condition of rf power and gas pressure, 4.8 W and 0.084 Torr, respectively. This minimized the discharge noise. This condition was attainable only from a discharge with a larger rf power, due to the hysteretic characteristics of the discharge. A pick-up coil wound around the tube and a capacitor formed a tank circuit with a  $Q$ -value of about 20, adjusted to be resonant with the rf frequency. The OG signals were thus the laser-induced changes in the rf

current picked up by the coil. The dye LDS 820 (Exciton) was pumped with all lines of an  $\text{Ar}^+$  laser. At a pump power of 4 W, a peak output of 250 mW was available from the dye laser equipped with a birefringent filter (BRF). The dye laser had typically a  $0.7 \text{ cm}^{-1}$  linewidth and was scanned by rotating the BRF. The laser beam, mechanically chopped at a frequency of 3.6 kHz, was subsequently directed and focused onto the center of the discharge tube.

The optogalvanic signal of  $\text{O}^-$  is reproduced in Fig. 1 from [12]; it was obtained with a lock-in time constant of 1 s. The signal intensity was normalized with respect to the incident laser power using a ratio meter. Six thresholds resulting from the fine structure transitions [12]  $\text{O}^-(^2P_{3/2,1/2}) + h\nu \rightarrow \text{O}(^3P_{2,1,0}) + e^-$  are indicated in the figure. Scan (B) shows that the OG signal is still nonzero at frequencies below the onset of the  $^2P_{1/2} \rightarrow ^3P_2$  transition. This signal is considered to be due to photodetachment of  $\text{O}_2^-$  for which the electron affinity is 0.44 eV [4].

The dependence of the OG signal on laser power, measured for the same discharge condition described above, is shown in Fig. 2. In this measurement, red laser light from a  $\text{Kr}^+$  laser (647 and 676 nm) was employed and was directed through the discharge. Transmitted laser power was monitored with a Scientech power meter and the laser power was varied with absorption filters. The OG signal was linearly proportional to the laser power up to 1.5 W.

The rf induced rms voltage  $V_{\text{rms}}$  across the pick-up coil was 40 V for an input power of 4.8 W. There was a considerable rf voltage across the pick-up coil even without a discharge, which might be coupled through the rf radiation. The signal-to-noise ratio (SNR) at a laser frequency of  $12200 \text{ cm}^{-1}$  was approximately 500 at a detector bandwidth of 0.3 Hz. Maximum SNR for  $\text{O}^-$  detection was obtained in an rf discharge in which the optogalvanic signal due to the oxygen atom was hardly observed in the energy range studied, contrary to the other type of discharges discussed below.

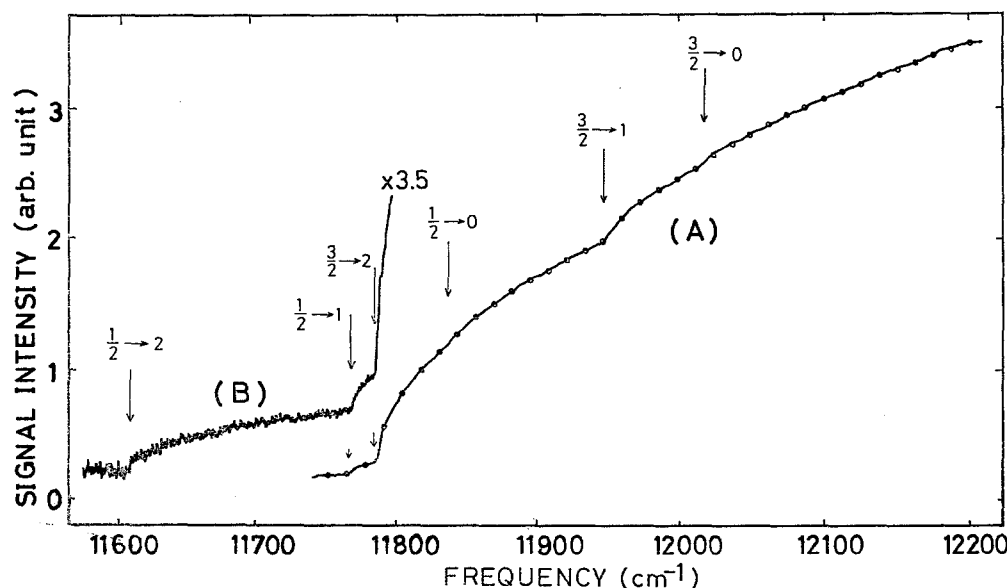


Fig. 1. Optogalvanic spectrum for photodetachment of oxygen in a rf discharge. The six fine-structure thresholds for transitions  $^2P_{J'} \rightarrow ^3P_J$  are marked by arrows and labelled  $J' \rightarrow J$ . Trace (B) is recorded with 3.5 times greater sensitivity. The OG signal at frequencies below  $11600 \text{ cm}^{-1}$  is due to  $\text{O}_2^-$  photodetachment

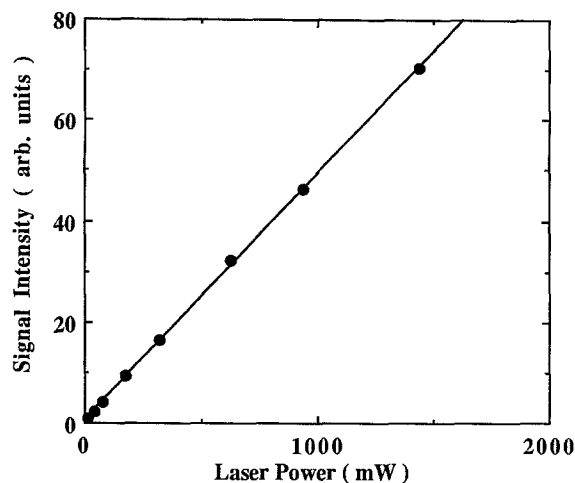


Fig. 2. Dependence of OG signal amplitude on laser power. The points correspond to experimentally measured values and the line is a least-squares fit

### 1.2. Microwave Discharge

The experimental arrangement for OG detection in the microwave discharge has been described previously [17]. Briefly, microwave radiation at a frequency of 2.45 GHz generated by a magnetron was fed into the microwave cavity (Evenson type) through a coaxial cable. The discharge tube is a Pyrex glass tube of 12 mm outside diameter. Two tungsten wires (0.5 mm diameter and 30 mm length), placed parallel to the tube wall, were used as probes for OG detection. When the discharge was sustained, a potential difference of up to several volts appeared across the two probes due to an inhomogeneous plasma distribution inside the cavity. The OG signal was measured as a change in the voltage difference between the two probes. When a bias voltage of several volts was applied across the probes, there was an increase in the signal intensity with a more or less similar SNR.

The microwave power was adjusted to minimize discharge noise. Residual noise at a discharge condition of minimum noise were recognized to be caused by magnetron noise [17]. The OG signal was recorded over the tuning range of rhodamine 6G without a correction for the varying laser output which has a maximum power of 0.4 W around  $16\,600\text{ cm}^{-1}$ . Figure 3 shows the typical OG signal of an oxygen discharge obtained at a pressure

of 0.6 Torr and a microwave power of 20 W with laser-irradiation through the sheath region close to the probe surface. The SNR was not critically dependent on microwave power. We could not get a better SNR than in the rf discharge. OG signals of atomic oxygen together with a broad continuum due to the photodetachment of negative oxygen ions were always observed. Assignment of the transitions of atomic oxygen shown in Fig. 3 were derived directly from listed transition frequencies [18], and are transitions originating from  $3p$  levels, which are about 9 eV above the ground state of atomic oxygen.

### 1.3. Hollow Cathode DC Discharge

The optogalvanic signal of  $\text{O}^-$  was also observable in a hollow cathode discharge using laser light from the rhodamine 6G dye laser. We used a commercial Ti hollow cathode lamp (HTV, L2783) filled with a mixed gas containing equal amounts of  $\text{O}_2$  and Ne at a total pressure of 6 Torr. The minimum discharge current was 9 mA at a tube voltage of 340 V. The OG signal decreased with increasing the discharge current. Discharge noise was also larger at a smaller current. No appreciable OG signal due to  $\text{O}^-$  was observed when the discharge current was increased beyond 15 mA.

The OG signal due to transitions between excited levels of neutral atomic oxygen was also observed when the laser irradiated the vicinity of the cathode surface. The ratio of OG signals for negative ions and atomic oxygen were dependent on the position of laser irradiation. The OG signal due to the photodetachment of  $\text{O}^-$  was intense at the center of the discharge tube, whereas the OG signal of atomic oxygen was intense in the vicinity of the cathode surface, where the OG signal of  $\text{O}^-$  was hardly observable.

### 1.4. Other Molecules

We observed similar continuum OG signals from a discharge of several kinds of molecular gases for conditions as listed in Table 1. For this measurement, we introduced various gases into the discharge region of either a microwave discharge or an rf discharge as described above. We used a laser light, either from Rh6G

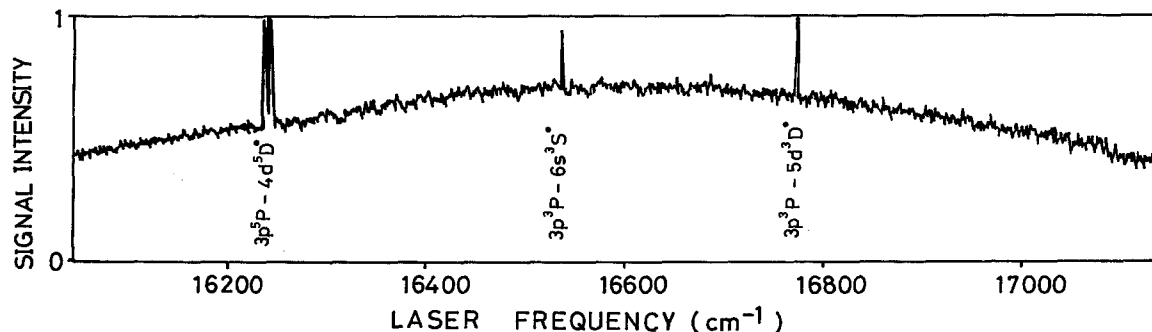


Fig. 3. Optogalvanic spectrum for photodetachment of oxygen in a microwave discharge. The OG signals of atomic oxygen originate in the transitions from the triplet  $3p$  levels

**Table 1.** Molecular species for which OG signals were recorded

	RF discharge <sup>a</sup>		Microwave discharge <sup>b</sup>	
	Pressure [Torr]	Input power [W]	Pressure [Torr]	Input power <sup>c</sup> [W]
O <sub>2</sub>	0.084	4.8	0.6	20
H <sub>2</sub>	0.2	8.5	0.2	20
H <sub>2</sub> O <sub>2</sub>	0.15	4.5	0.1	20
CO	– <sup>d</sup>	–	0.53	20
(COCH <sub>3</sub> ) <sub>2</sub>	0.07	4.0	0.2	20

<sup>a</sup> Red light from Kr<sup>+</sup> laser (647, 676 nm) was used

<sup>b</sup> Yellow light from Rh6G dye laser was used

<sup>c</sup> OG signal was not critically dependent on the input microwave power

<sup>d</sup> Not tested

dye laser around 590 nm or, Kr<sup>+</sup> laser at 647 or 676 nm. We recorded continuum OG signals for H<sub>2</sub>, biacetyl (COCH<sub>3</sub>)<sub>2</sub>, H<sub>2</sub>O<sub>2</sub>, and CO. A prolonged operation of the discharge was hindered due to the deposition of a carbon film in a discharge containing carbon atoms, which finally caused an unstable discharge to occur. The discharge was usually rather noisy and the SNR was, typically, as low as 10. The SNR increased slightly when argon gas was added as a buffer gas. The signal, although most probably due to the photodetachment of either H<sup>−</sup> or O<sup>−</sup> and O<sub>2</sub><sup>−</sup>, was not studied further to identify its origin. Negative ions possibly existing in the discharge are O<sup>−</sup> (1.46), O<sub>2</sub><sup>−</sup> (0.44), H<sup>−</sup> (0.75), OH<sup>−</sup> (1.83), CH<sup>−</sup> (1.24) etc., where the values in parentheses represent the electron affinity [19]. We were not successful, under the present experimental conditions, in observing OG signals from other molecules such as CF<sub>4</sub>, SF<sub>6</sub>, CH<sub>3</sub>CHO, (CH<sub>3</sub>)<sub>2</sub>CO, CH<sub>2</sub>Cl<sub>2</sub>, and CHCCl<sub>3</sub>.

## 2. Results and Discussions

The linear dependence of the OG signal on laser power shown in Fig. 2 suggests that there is no optical saturation within the available laser power and indicates that laser interaction can be treated as a small perturbation. The signal amplitude may thus be proportional to changes in discharge parameters caused by laser photodetachment and is estimated in the following.

Although we did not measure the discharge parameters directly, an order of magnitude calculation was possible from the intensity of the OG signal. Experimentally, an effective SNR of 300 for a unit detector bandwidth was obtained at a laser wavelength of 820 nm, with a laser power of 250 mW and a laser diameter of 1 mm. So long as the density of the photodetached electrons is a small fraction of the steady state value, it can reasonably be assumed that the OG signal is linearly proportional to the number of the photodetached electrons. Released electron flow may thus be approximated as the shot-noise current times the SNR, since the minimum detectable variation in the discharge current observed in the OG signal is ultimately determined by the shot noise of the discharge under the least noisy discharge conditions [16]. The negative ion density estimated here should therefore be

taken as a lower limit, since the observable SNR is likely to be larger for an ideal least-noisy discharge.

The shot noise current was estimated from the rf induced rms voltage  $V_{\text{rms}}$  of 40 V for an input rf power of 4.8 W measured across the pick-up coil with an inductance  $L$  of  $1.4 \times 10^{-6}$  H and which formed a tank circuit with a  $Q$ -value of 20. When the whole rf field of frequency  $\omega$  was coupled through the discharge current, the rms discharge current  $I_{\text{rms}}$  obtained from  $I_{\text{rms}} = V_{\text{rms}}/L\omega Q$  was 17 mA. The rms shot-noise current  $I_n$  in a bandwidth  $B$  due to a current  $I_t$  is  $I_n = (2eI_t B)^{1/2}$ . The shot noise current was calculated to be  $7.3 \times 10^{-11}$  A for a unit bandwidth; the corresponding electron rate was  $4.6 \times 10^8 \text{ s}^{-1}$  from the relation. Thus, the increasing rate of electron number  $\Delta N_e$  due to the photodetachment of O<sup>−</sup> in an interaction length  $l$  should be

$$\Delta N_e = P_{\text{laser}} \sigma_{\text{det}} n_{\text{O}^-} l / h\nu$$

where  $P_{\text{laser}}$  is the laser power,  $\sigma_{\text{det}}$  the photodetachment cross section,  $n_{\text{O}^-}$  the O<sup>−</sup> density,  $h$  is Planck's constant and  $\nu$  the laser frequency. This will give  $n_{\text{O}^-} = 1.1 \times 10^{10} \text{ cm}^{-3}$  using  $\sigma_{\text{det}} = 2.5 \times 10^{-18} \text{ cm}^2$  [20] and an interaction length of 5 cm. This value is, to our knowledge, the first determination of the oxygen negative ion density in rf discharge. In a hollow cathode dc discharge, a value of  $6 \times 10^8 \text{ cm}^{-3}$  was obtained by the probe method [15].

The change in the electron density  $\delta n_e$  will be given from the relation  $\Delta N_e = \delta n_e v_d S$ , where  $v_d$  is the electron drift velocity and  $S$  the cross section of the interaction region. Then  $\delta n_e$  is calculated to be  $1.7 \times 10^6 \text{ cm}^{-3}$  for an electron drift velocity of  $10^7 \text{ cm/s}$  [21] estimated for an electric field of 10 V/cm [12]. On the other hand, the steady state electron density in our case is  $5 \times 10^8 \text{ cm}^{-3}$  if it is 1/20 of the negative ion density, as has been found in a dc discharge [15]. Thus, the photodetached electron density obtained is three orders of magnitude smaller than the steady state value. This is consistent with the observed linearity of the laser-power dependence of the OG signal shown in Fig. 2. When the density of the photodetached electrons becomes comparable to the steady state value, we have to take into account changes in dynamics of the discharge. From the above discussion it is clear that the optical saturation, i.e., the depletion of the negative ions caused by absorption of laser, will be negligible here since

the negative ion density is still one order of magnitude larger than the electron density.

In a hollow cathode dc discharge, the OG signal due to oxygen atoms was obtained by irradiation near the cathode surface, while the corresponding signal was not observable in the positive column like in an rf discharge as shown by Fig. 1. The OG signal observed in a microwave discharge had a similar behavior to the one observed in the cathode fall region of the dc discharge. The lack of any atomic spectra within the frequency range studied in the positive column or in an rf discharge is due to the small population of excited oxygen atoms; the abundant negative ions there, are a result of the predominant mechanism of negative ion formation by the dissociative attachment, which has a larger cross section for slower electrons. In the cathode fall region of the dc discharge, high-energy electrons causes electron impact excitation or ionization, leaving a lower population of fragile negative ions and a considerable population of excited oxygen atoms. A similar mechanism applies in the sheath region in our experiment with the microwave discharge.

The OG signal for negative ions observed in the positive column has been shown to be proportional to the laser power. The signal intensity can be estimated from a simplified model using discharge parameters. This shows, when combined with another method like the Langmuir-probe method [17] which gives absolute values of the discharge parameters, that the OG method can be used as a plasma diagnostic technique.

OG signals due to negative ions have also been observed in discharges of several kinds of gases. Further efforts to find better discharge conditions are clearly necessary in order to identify negative ion species, together with the use of a laser of appropriate wavelength. The simple experimental system for the OG detection of negative ions described here will also be useful for the study of fundamental processes of charged particles in various discharge plasmas.

*Acknowledgement.* We have benefited greatly from instructive and stimulating conversations with Dr. H. Amemiya.

## References

1. H.S.W. Massey: *Negative Ions*, 3rd edn. (Cambridge University Press, London 1976)
2. D.P. Sheehan, N. Rynn: *Rev. Sci. Instrum.* **59**, 1369 (1988)
3. J.W. Coburn: *Plasma Chem. Plasma Proc.* **2**, 1 (1982)
4. R.B. Green, R.A. Keller, G.G. Luther, P.K. Schenck, J.C. Travis: *IEEE J. QE-13*, 63 (1977)
5. C.R. Webster, C.T. Rettner: *Laser Focus* (Feb. 1983) and references therein
6. See, for example, R.A. Gottsho, T.A. Miller: *Pure Appl. Chem.* **56**, 189 (1984)
7. C.R. Webster, I.S. McDermid: *J. Chem. Phys.* **78**, 646 (1983)
8. R. Klein, R.P. McGinnis, S.R. Leone: *Chem. Phys. Lett.* **100**, 475 (1983)
9. I.S. McDermid, C.R. Webster: *J. de Phys. Colloq.* **44**, C7-461 (1983)
10. R.A. Gottsho, C.E. Gaebe: *IEEE Trans. PS-14*, 92 (1986)
11. J. Kramer: *J. Appl. Phys.* **60**, 3072 (1986)  
G.L. Rogoff, J.M. Kramer, R.B. Piejak: *IEEE Trans. PS-14*, 103 (1986)
12. T. Suzuki, T. Kasuya: *Phys. Rev. A* **36**, 2129 (1987)
13. A.R.P. Rau, U. Fano: *Phys. Rev. A* **4**, 1751 (1971)
14. F.K. Kaufman: *Adv. Chem. Ser.* **80**, 29 (1969)
15. J.B. Thompson: *Proc. R. Soc. Lond. A* **262**, 503 (1961); **A 262**, 519 (1961)
16. T. Suzuki: *Opt. Commun.* **38**, 364 (1981);  
T. Suzuki, M. Kakimoto: *J. Mol. Spectrosc.* **93**, 423 (1982)
17. H. Sekiguchi, A. Masuyama, T. Kasuya, T. Suzuki: *J. Appl. Phys.* **58**, 154 (1985);  
T. Suzuki, H. Sekiguchi, T. Kasuya: *J. Phys. (Paris) Colloq.* **44**, C7-419 (1983)
18. C.E. Moore: *Nat. St. Ref. Data Ser.* **3**, Sect. 7 (1975)
19. A.A. Radzig, B.M. Smirnov: *Reference Data on Atoms, Molecules, and Ions* (Springer, Berlin, Heidelberg 1985)
20. L.M. Branscomb, D.S. Burch, S.J. Smith, S. Geltman: *Phys. Rev.* **111**, 504 (1958)
21. D.R. Nelson, F.J. Davis: *J. Chem. Phys.* **57**, 4070 (1972)